Korean J. Chem. Eng., **19**(4), 703-710 (2002)

Effect of Microbubbles and Particle Size on the Particle Collection in the Column Flotation

Jung-Eun Lee and Jae-Keun Lee*†

HydroLab Institute, Sum-Jin EST Company, Songjeong-Dong, Gangseo-Gu, Busan 618-270, Korea
*Department of Mechanical Engineering, Pusan National University, Busan 609-735, Korea
(*Received 4 October 2001 • accepted 28 January 2002*)

Abstract−Particle-bubble collection characteristics from microbubble behavior in column flotation have been studied theoretically and experimentally. A flotation model taking into account particle collection has been developed by particle-bubble collision followed by the particle sliding over the bubble during which attachment may occur. Bubble size and bubble swarm velocity were measured as a function of frother dosage and superficial gas velocity to estimate the collision and collection efficiency. Separation tests were carried out to compare with theoretical particle recovery. Fly ash particles in the size range of <38, 38-75, 75-125, >125 μm were used as separation test particles. Theoretical collision and collection efficiencies were estimated by experimental data on the bubble behavior such as bubble size, gas holdup and bubble swarm velocity. Collection efficiency improved with an increase of the bubble size and particle size but decreased in the particle size up to 52 μm. Also, flotation rate constants were estimated to predict the optimum separation condition. From the theoretical results on the flotation rate constant, optimum separation condition was estimated as bubble size of 0.3-0.4 mm and superficial gas velocity of 1.5-2.0 cm/s. A decrease of bubble size improved the collection efficiency but did not improve particle recovery.

Key words: Flotation, Particle, Bubble, Collision Efficiency, Collection Efficiency, Flotation Rate Constant

INTRODUCTION

Flotation is regarded as the best available technique for separating fine particles. In flotation particles and bubbles are generally moving in opposite directions. The collection process can be studied by considering a gas bubble rising through a dilute slurry. Collision is the fraction of all particles swept out by the projected area of the bubble that collide with the bubble. Subsequent to collision a particle will move along the bubble surface with a sliding motion. The sliding particle maintains bubble contact until the fluid streamlines carry it radically away from the bubble surface, unless attachment occurs prior to this. Attachment is the fraction of all colliding particles that undergo successful attachment during the time of contact. Collision has been modeled and showed that a smaller bubble increases collision efficiency because bubble velocity decreases with smaller bubble size [Weber et al., 1983; Jiang et al., 1986]. Attachment has received less attention than has collision. A notable early theoretical study was that of Sutherland [Sutherland, 1948], and the attachment has been examined recently by Dobby and Finch [Doby et al., 1986].

The overall rate of flotation in a practical particle separation depends on so many factors that it is not yet possible to attempt a fundamental calculation of the kinetics. The particle recovery depends not only on the solids content of the pulp and the hydraulic regimes in the cell, but also on the size distribution of the particle, the bubble population, and concentration of frother [Tuteja et al., 1995; Bergh et al., 1993]. But particle size and bubble size are believed to be the dominant physical factors in the flotation. Microbubbles are desirable for fine particle flotation because they increase particle-bubble collision probability [Yoon, 1993]. But the generation of very small gas bubbles has not always yielded higher flotation rate constants [Doby et al., 1986].

The purpose of this study is to present an investigation of the particle-bubble collection characteristics experimentally and theoretically. Bubble size, gas holdup and bubble swarm velocity were measured to estimate the particle-bubble collection theoretically. From the theoretical results on the particle-bubble collection characteristics, optimum separation condition such as bubble size and superficial gas velocity was presented. Particle separation tests were carried out to compare with the theoretical particle-bubble collection characteristics.

THEORY

1. Collection Model

Particle collection is considered to occur by particle collision followed by the particle sliding over the bubble surface. Collision is quantified by collision efficiency (E_C) for gravitation and interception of spherical particles on the bubble. Attachment is quantified by an attachment efficiency (E_A) calculated as the fraction of particles which reside on the bubble for a time greater than the induction time. Collection efficiency (E_K) was given as follows [Weber et al., 1983; Doby et al., 1986].

$$E_K = E_C \cdot E_A \tag{1}$$

The assumption of bubbles acting as rigid spheres is reasonable in the surfactant solutions used in flotation. Particles are assumed to be spherical and shape corrections are not employed. Collection efficiency is directly proportional to the flotation rate constant [Clift

†To whom correspondence should be addressed.
E-mail: jklee@pusan.ac.kr

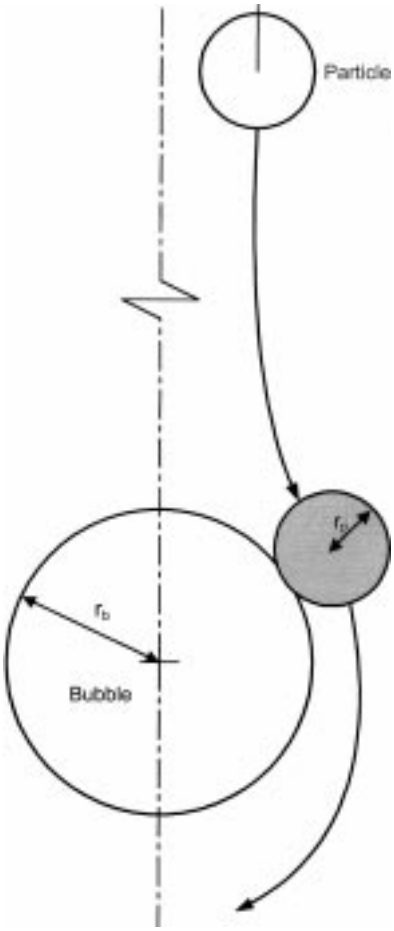

Fig. 1. An illustration of a particle approaching at a gas bubble [Jiang, 1986].

et al., 1978; Finch et al., 1990].

2. Collision Model

Fig. 1 illustrates a particle approaching a bubble [Jiang et al., 1986; Finch et al., 1990]. In the system shown in Fig. 1 the bubble is held stationary at the origin of the coordinates by a downward fluid flow equal to the freely rising velocity of the bubble. Thus, the forces acting on the particle are inertial force, drag force, gravitational force and buoyant force. The equations of motion in the x and y direction are given by [Finch et al., 1990].

$$Sk\frac{d\hat{v}_x^*}{dt^*} = u_x^* - v_x^* \tag{2}$$

$$Sk\frac{dv_y^*}{dt^*} = u_p^* + u_y^* - v_y^* \tag{3}$$

where Sk is the Stokes number, given by

$$Sk = \frac{1}{9}\left(\frac{\rho_p}{\rho_l}\right)\left(\frac{r_p}{r_b}\right)^2 Re_b \tag{4}$$

$u_{x,y}$ and $v_{x,y}$ are liquid and particle velocities, respectively, and u_p^* is the particle terminal velocity, all made dimensionless by dividing by the bubble rise velocity, u_b. t^* is time made dimensionless by multiplying by (u_b/d_b). Particle terminal velocity is calculated assuming Stokes' equation:

$$u_p = g(\rho_p - \rho_l)d_p^2/(18\mu_l) \tag{5}$$

The Stokes number is related to the ratio of inertial to drag forces. Most work has focused on conditions where Sk<<1 and thereby allowing this inertial term to be ignored.

2-1. Low Particle Inertia, Sk<0.1

In the collision model of Weber and Paddock, which assumes Sk=0, total collision efficiency is the sum of gravitational and interceptive collision [Weber et al., 1983].

$$E_C = E_{Cg} + E_{Ci} \tag{6}$$

Interceptional collision alone (E_{Cg}=0) occurs for neutrally buoyant particles which follow the fluid streamlines exactly. Gravitational collision alone (E_{Ci}=0) is hypothetical; it would occur for particles having a finite settling velocity but zero dimension. Interceptional collision is given by [Weber, 1983]:

$$E_{Ci} = \frac{1.5}{1+u_p^*}\left(\frac{d_p}{d_b}\right)^2\left[1+\frac{(3/16)Re_b}{1+0.249Re_b^{0.56}}\right] \tag{7}$$

for $0<Re_b\leq 300$. Gravitational collision is given by [Reay, 1973]:

$$E_{Cg} = \frac{u_p^*}{1+u_p^*}\left(1+\frac{d_p}{d_b}\right)^2 \sin^2\theta_c \tag{8}$$

where θ_c is the angle (from the front stagnation point of the bubble) where the fluid streamlines come closest to the bubble. θ_c has been fitted to the results of Woo [Woo, 1971]:

$$\theta_c = 7.81 - 7.37\log Re_b \quad (20<Re_b<400) \tag{9a}$$

$$\theta_c = 98.0 - 12.49\log(10Re_b) \quad (1<Re_b<200) \tag{9b}$$

$$\theta_c = 90.0 - 2.5\log(100Re_b) \quad (0.1<Re_b<1) \tag{9c}$$

2-2. Intermediate Particle Inertia, Sk>0.1

Collision efficiencies for Sk>0.1 have been calculated by determining particle trajectories by using a numerical solution to the equation of motion [as shown in Eqs. (2) and (3)] and finding the grazing trajectory by trial-and-error. Collision efficiency is estimated from the following correlation [Finch et al., 1990]:

$$E_C = E_{C0}(1.63Re_b^{0.06}Sk^{0.54}u_p^{*-0.16}) \quad (Sk>0.1) \tag{10}$$

where E_{C0} is the collision efficiency obtained from Eq. (6) for conditions where Sk<0.1.

3. Attachment Model

The underlying assumption is that after collision the particle slides over the bubble and attachment occurs when the intervening liquid film thins and ruptures. The time required for the film to rupture is the induction time, t_i. Consequently, particles with a sliding time greater than induction time are considered to have attached.

3-1. Particle Sliding Time

The calculation of particle sliding time, t_s requires a knowledge of (a) the distribution on the bubble surface of particle collision angles, (b) the angle at which fluid streamlines start to carry the particle radially away from the bubble, i.e., the maximum angle of contact θ_m, and (c) the particle sliding velocity.

The distribution is quantified by the fraction of all colliding particles that collide between the front stagnation point and some angle θ.

$$n_\theta = \frac{\sin^2\theta}{\sin^2\theta_c} \quad (11)$$

where θ_c is given by Eq. (9). θ_m is calculated by determining the angle at which the radial component of the particle settling velocity is equal to the radial component of the liquid velocity. At $\theta > \theta_m$ the particle no longer contacts the bubble, unless attachment has already occurred. A correlation between θ_m, ρ_p and θ_c is given by [Finch et al., 1990]:

$$\theta_m = 9 + 8.1\rho_p + \theta_c(0.9 - 0.09\rho_p) \quad (12)$$

Particle sliding velocity v_θ over the bubble surface is the sum of the tangential component of particle settling velocity, $u_p \sin\theta$, and the local tangential liquid velocity. For $d_p/d_b < 0.03$ particle sliding velocity is given by [Dobby et al., 1986]:

$$u_{p\theta} = 0.7\xi_s u_b \frac{d_p}{d_b} + u_p \sin\theta \quad (13a)$$

where the surface vorticity ξ_s has been estimated by correlating with θ and Re_b. For $d_p/d_b > 0.03$ the particle velocity is calculated by dividing the particle into two zones, the lower part that sees a velocity gradient and the upper part that sees a constant velocity.

$$u_{p\theta} = 0.7\xi_s u_b \left[\frac{(d_p - 0.03d_b)}{d_p} 0.06 + \left(\frac{0.03d_b}{d_p}\right) 0.03\right] + u_p \sin\theta \quad (13b)$$

Thus, the particle sliding time can now be calculated as follows,

$$t_s = \left(\frac{\theta_m - \theta}{360}\right) \pi (d_p + d_b)/\bar{u}_{p\theta} \quad (14)$$

where $\bar{u}_{p\theta}$ is the average particle sliding velocity, determined from Eq. (13) using average values of ξ_s and $\sin\theta$.

3-2. Attachment Efficiency

A particle attaches to a bubble when the sliding time t_s equals or exceeds the induction time t_i. Let θ' be the angle θ in Eq. (14) when $t_s = t_i$. After rearrangement this gives [Finch et al., 1990]:

$$\theta' = \theta_m - \frac{360 u_{p\theta} t_i}{\pi(d_b + d_p)} \quad (15)$$

Consequently, attachment efficiency is given by:

$$E_A = \frac{\sin^2\theta'}{\sin^2\theta_c} \quad (16)$$

4. Collection in a Bubble Swarm

To this point the model is a single bubble model. It is intuitive that there would be interaction between bubbles in a bubble swarm. The data of LeClair were fitted by a polynomial regression of the form [LeClair, 1970]:

$$\xi_{se} = \xi_s + n\varepsilon_g \quad (17)$$

where ξ_{se} is the surface vorticity of a bubble at gas holdup ε_g and n is a function of Re_b and θ.

An increase in gas holdup increases collection efficiency. The principal reason is the decrease in bubble swarm velocity. One way to increase ε_g is to increase gas rate. However, this will be also cause d_b to increase. Flotation rate constant is related to E_K by:

$$k_c = 1.5 \frac{J_g E_K}{d_b} \quad (18)$$

Consequently, the flotation rate constant may be pass through a maximum with J_g as the effect of increasing the number of bubbles is progressively offset by an increasing d_b and (consequently) decreasing E_K. Recovery of a particle in the collection zone is given by:

$$R = 1 - \exp(-k_c t_p) \quad (19)$$

where t_p is the residence time of the particle in the collection zone. Eqs. (18) and (19) provide a link between E_K, k_c, and R. Therefore, a fundamental analysis of the collection process that provides relationships between E_K and process parameters, such as particle size and bubble size, can be extended to provide relationships between R (or k_c) and process parameters.

EXPERIMENTAL METHODS

1. Bubble Behavior Measurements

Bubble behavior such as bubble size, gas holdup and bubble swarm velocity is needed to evaluate the collision and collection efficiency between particle and bubble. Fig. 2 is the experimental apparatus to measure bubble size, gas holdup and bubble swarm velocity. The experiments were conducted in a column with inner diameter of 9 cm and height of 240 cm. A given dosage of frother (MIBC : Methyl Iso Butyl Carbinol) was added into, and mixed with 30 L of tap water in a conditioning tank for about 1,800 sec. The solution was pumped into the column. The gas was introduced and controlled by an air regulator (TPC, TAR 4000) and a rotameter (Dwyer, RMA).

1-1. Bubble Size

Microbubbles were generated with the in-line mixer, and bubble size was controlled by a variety of superficial gas velocity and frother dosage. A Plexiglas box filled with water was placed around the column for photographic measurement of bubble size. The water-

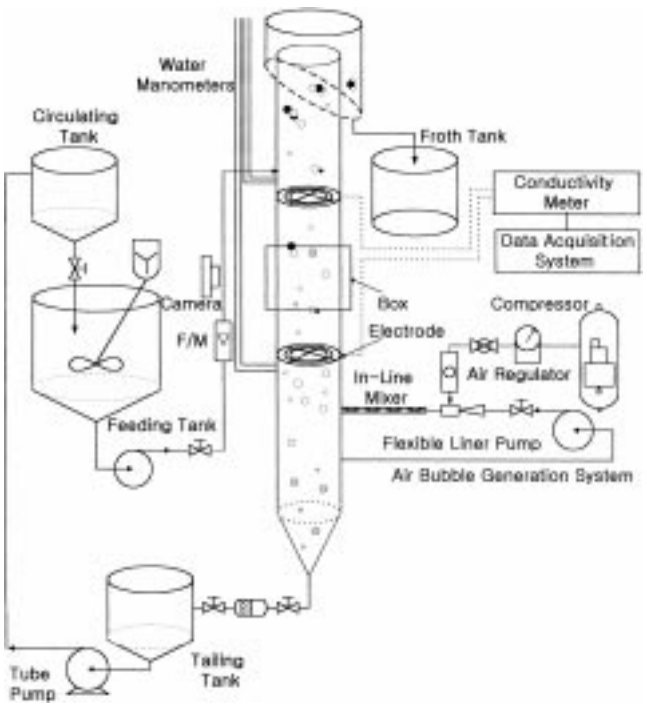

Fig. 2. Schematic diagram of experimental apparatus for flotation.

filled box reduces optical distortion due to the curved wall of the column. Bubble size distributions and bubble shapes were determined by using ten times enlargement. Counting and measurement of bubble sizes were done manually or automatically by using an image analyzer. A minimum of 400 bubbles was counted. The average bubble size was estimated as the Sauter mean diameter as it is considered the most consistent representation of mean bubble size [Yianatos et al., 1988; Patel et al., 1990].

$$d_{bs}=\frac{\sum n_i d_{bi}^3}{\sum n_i d_{bi}^2} \tag{20}$$

where d_{bi} and n_i are the corresponding bubble diameter and number of bubble, respectively.

1-2. Gas Holdup

Gas holdup is one of the most important parameters characterizing the hydrodynamics of the column flotation. It can be defined as the percentage by volume of the gas in the two or three phase mixture in the column. Water manometers were used to measure the gas holdup given by [Lee, 1999]:

$$\varepsilon_g=\frac{\Delta h}{\Delta L} \tag{21}$$

where Δh is the distance between the water level in the two manometers, and ΔL is the distance between the location of the manometers.

1-3. Bubble Swarm Velocity

A conductivity technique was used to measure the bubble swarm velocity [Uribe et al., 1994]. Two grid electrodes covering the cross-sectional area of the column were used. The grid electrode consisted of three concentric rings soldered to a cross. Copper wire of 0.14 cm diameter was used. The grid electrodes were located one above the other along the vertical axis of the column. The conductivity measurements were performed with a conductivity meter (YSI, Model 3200). When the air flow was terminated, an interface appeared: above the interface the gas holdup was that prior to the termination of the air flow; below the interface the gas holdup was zero. Fig. 3 presents a typical rising curve of the interface. As readily observed in Fig. 3, when the air flow is terminated, the curves present three different stages: stage ①, when the rising interface is not reaching the lower electrode and the conductivity is constant; stage ②, when the interface moves between the two electrodes; and stage ③, when the interface leaves the upper conductivity and the conductivity is again constant. Therefore, the bubble swarm velocity is given by [Lee, 1999]:

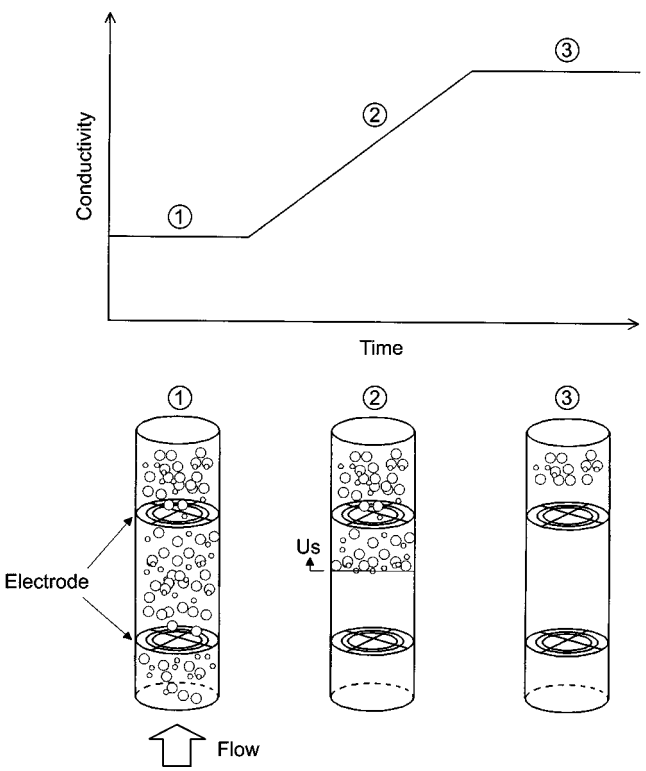

Fig. 3. Fundamental concept for measuring bubble swarm velocity between two electrodes [Lee, 1999].

$$U_s=\frac{\Delta L_e}{\Delta T} \tag{22}$$

where ΔL_e is the distance between two electrodes and ΔT is the time that interface rises between two electrodes.

2. Particle Separation Test

Fly ash particles in the size range of <38, 38-75, 75-125, and >125 μm were used as separation test particles. The size distribution of the fly ash was determined by wet screening. Fig. 2 is the experimental apparatus for particle separation by flotation. Separation tests were carried out as described in Table 1.

In the flotation tests the slurry was prepared in 30 L of water, and was conditioned with collector (Kerosene) and frother (MIBC) for 1,800 sec. The slurry was pumped into the column and the hydrophobic particles in the slurry attach to the air bubbles. Hydrophobic particles are collected from the froth tank and loss-on-ignition tests were performed. Hydrophobic particles were normally predried in a laboratory oven at 130 °C for two hours, and after cooling and reweighing, were placed in an air ventilated laboratory oven at 740 °C for two hours. The change in weight between heating at 130 °C and 740 °C, divided by the original dry sample mass, was the reported LOI (Loss On Ignition). Experimental recovery was calculated as the fraction of particles that attach to gas bubbles and presented as Eq. (23).

$$R=\frac{\text{Separated particle weight}\times\text{LOI of separated particle}}{\text{Original particle weight}\times\text{LOI of original particle}} \tag{23}$$

Table 1. Test conditions for particle separation in column flotation

Parameters	Specification
Column diameter (cm)	8
Column length (cm)	240
Solid percent (%)	5
Superficial gas velocity (cm/s)	1.99
Air pressure (kg_f/cm^2)	1
Agitation (rpm)	1200
Conditioning time (sec)	1800
Frother dosage (mg/L)	300
Collector dosage (mg/L)	300
Sampling time (sec)	60

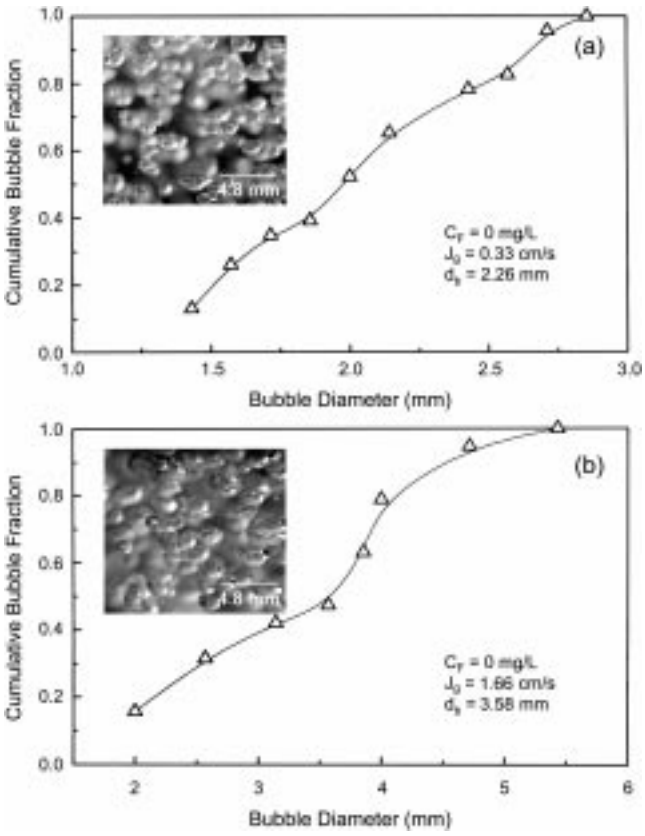

Fig. 4. Photographs and size distribution of air bubbles.
(a) C_F=0 mg/L, J_g=0.33 cm/s, (b) C_F=0 mg/L, J_g=1.66 cm/s

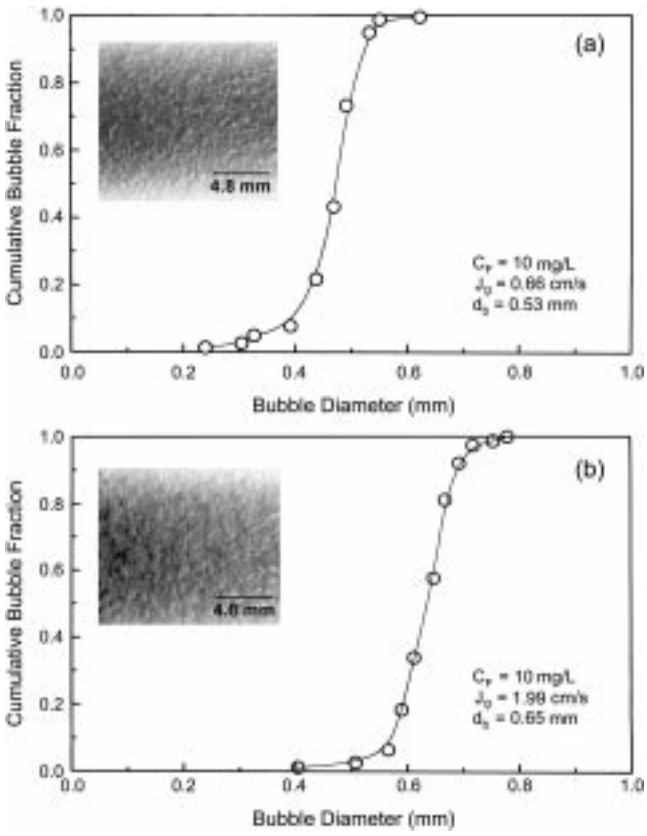

Fig. 5. Photographs and size distribution of air bubbles.
(a) C_F=10 mg/L, J_g=0.66 cm/s, (b) C_F=10 mg/L, J_g=1.99 cm/s

RESULTS AND DISCUSSION

1. Bubble Behavior

Photographs were taken in order to observe the shape of bubbles and determine the bubble size. In any experiments, photographs were taken in the bubbly zone as a function of flotation variables. Fig. 4 shows typical photographs of bubbles and bubble size distributions generated from the in-line mixer bubble generators with frother dosage of 0 mg/L and superficial gas velocities of 0.33 and 1.66 cm/s, respectively. Fig. 5 shows those with frother dosage of 10 mg/L and superficial gas velocities of 0.66 and 1.99 cm/s, respectively. From the photographs, bubble shapes are irregular something like to ellipsoidal and much larger without frother, but they are sphere shaped with frother dosage. Frothers are often employed to ensure the formation of bubbles with suitable size and stability in the flotation. One of the reasons for the increase of bubble size with the gas flowrate is related to the coalescence of bubbles, which depends on the resistance of the thin liquid film between bubbles to rupture. The ability to resist the rupture and coalescence of bubbles is stronger in the presence of frother than in the absence of frother [Zhou et al., 1993].

Fig. 6 presents the size distribution of bubbles as a function of superficial gas velocity and frother dosage, respectively. Fig. 6(a) shows the bubble size distributions under the conditions of 40 mg/L of frother dosage when the range of superficial gas velocity is 0.33-2.32 cm/s. When the frother dosage is constant, bubble size increases with increasing the superficial gas velocity. Fig. 6(b) shows the bubble size distributions with superficial gas velocity of 0.66 cm/s and the range of frother dosage of 40-300 mg/L. When the superficial gas velocity is constant, bubble size decreases with increasing the frother dosage.

From the experiments and Eq. (20), bubbles in the Sauter mean diameter of 0.26, 0.34, 0.42, 0.51, 0.59 and 0.67 mm were selected. In each experimental condition to acquire corresponding bubbles, gas holdup and bubble swarm velocity was measured. Table 2 presents the experimental conditions of bubble size, gas holdup and bubble swarm velocity in each condition.

2. Theoretical Results on the Collection Model

Collection efficiencies and flotation rate constants as a function of bubble size and particle size can be calculated by the experimental results of bubble behavior.

2-1. Bubble Size Effect

Fig. 7 is the collection efficiency as a function of bubble size. Decreasing bubble size clearly increases collection efficiency. This results from increases in both collision efficiency (as shown in Eqs. (7) and (8)) and attachment efficiency. The increase in the attachment efficiency is because the fractional decrease in particle sliding velocity on a smaller bubble exceeds the fractional decrease in sliding distance.

2-2. Particle Size Effect

Fig. 8 illustrates the relationship between collection efficiency and particle size. The first feature of note is that collection efficiency passes through a maximum in the particle size of 52 μm. The maximum is explained by the opposing effect of particle size upon

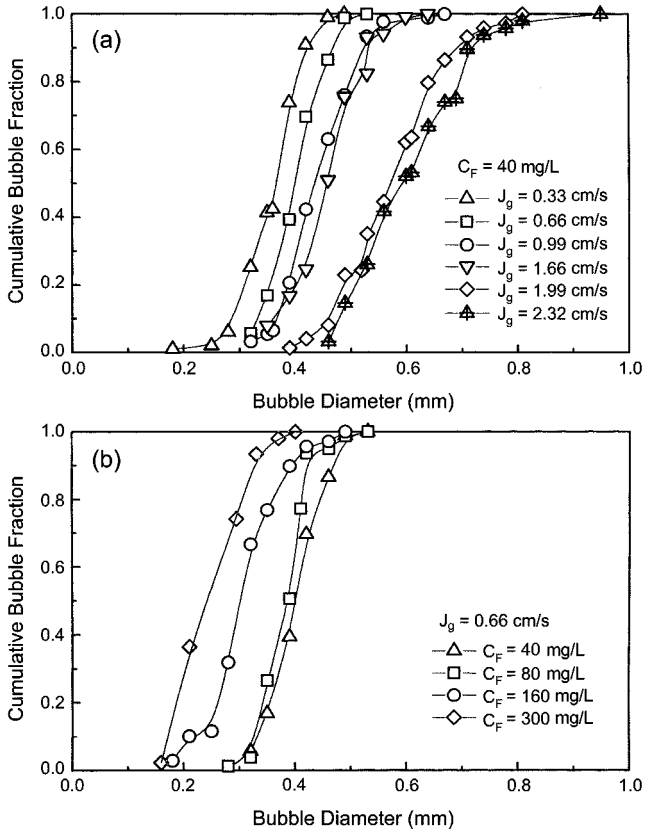

Fig. 6. Bubble size distribution as a function of (a) superficial gas velocity, (b) frother dosage.

Table 2. Test results of bubble size, gas holdup and bubble swarm velocity

C_F (mg/L)	J_g (cm/s)	d_b (mm)	ε_g	U_s (cm/s)
300	0.33	0.26	11.9	2.1
300	1.99	0.34	45.8	1.9
120	1.66	0.42	38.1	1.9
120	2.32	0.51	53.6	1.8
80	2.65	0.59	62.5	2.2
40	2.65	0.67	32.1	2.7

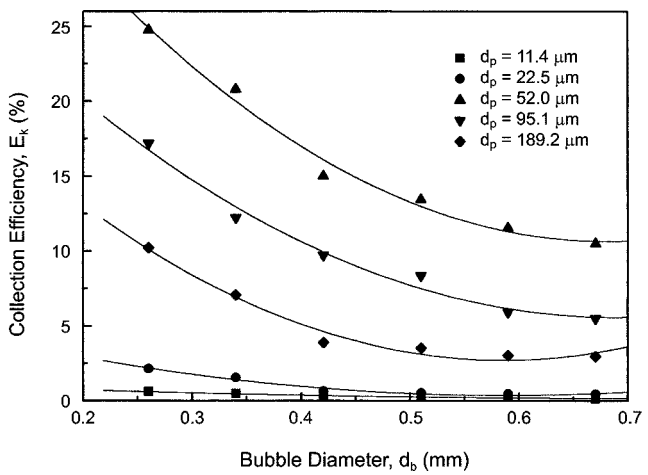

Fig. 7. Collection efficiency as a function of bubble size.

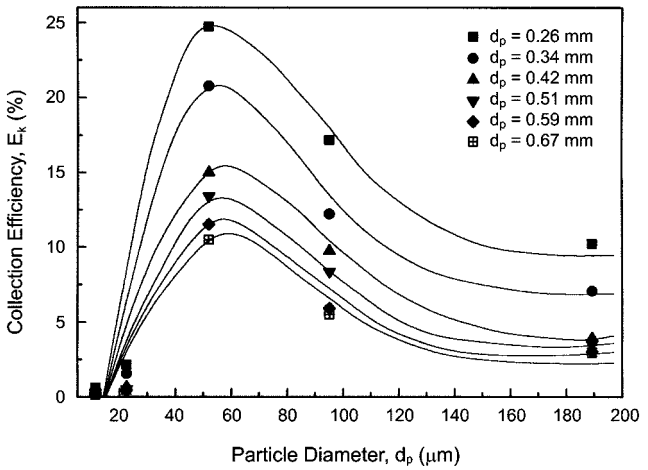

Fig. 8. Collection efficiency as a function of particle size.

collision and attachment: as particle size increases collision efficiency increases but attachment efficiency decreases. This is because large particles have a large velocity over the bubble and consequently particle sliding time decreases. Another reason is that particle gravity exceeds particle-bubble attachment with increasing particle size. That is, the gravity force of particle is greater than the attachment force between particle and bubble in the range of particle size more than 52 μm, which causes a decrease of attachment efficiency and therefore collection efficiency. But in the case of particle size less than 52 μm, collection efficiency is influenced by particle size as shown Eqs. (7) and (8), and therefore it is increased as a function particle size. Hence collection efficiency of particle more than 52 μm is controlled by gravity force, but it is influenced by attachment force in the case of particle less than 52 μm.

2-3. Optimum Condition

Fig. 9 is the flotation rate constant as a function of bubble size. Generally, decreasing bubble size increases flotation rate constant (as shown in Eq. (18)), but it has a maximum in the bubble size range of 0.3-0.4 mm. As a result, smaller bubbles increase collection efficiency but do not improve recovery. This is explained from Eq. (18) presented by [Finch, 1990]. Flotation rate (k_c) is determined

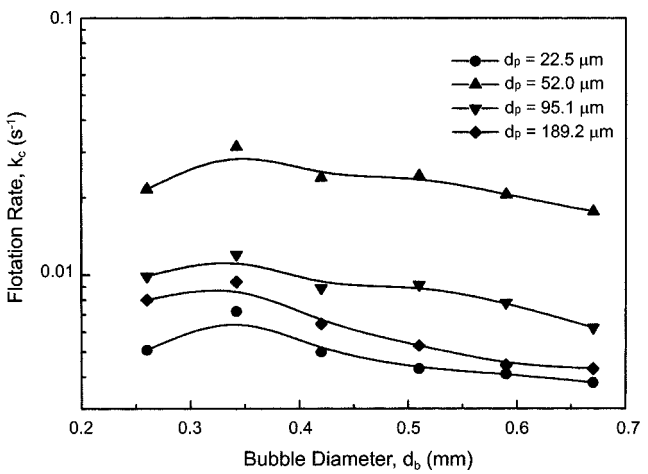

Fig. 9. Flotation rate constant as a function of bubble size.

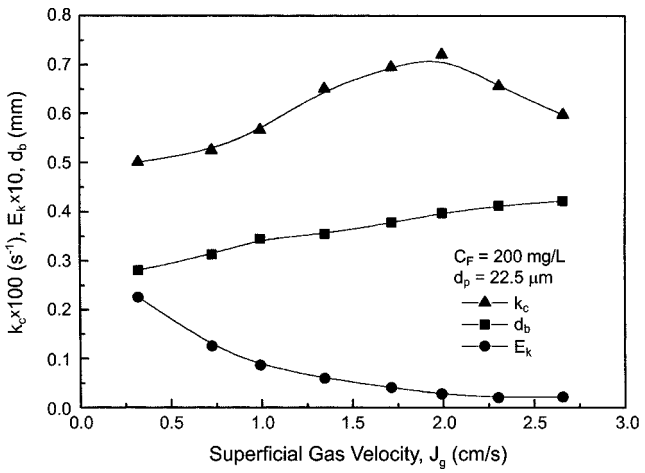

Fig. 10. Bubble size, collection efficiency and flotation rate as a function of superficial gas velocity for d_p=22.5 μm and C_F =200 mg/L.

by the bubble size (d_b) and the superficial gas velocity (J_g). It is typically tendency that k_c become decreased as bubble size is being increased, but in the range of 0.3-0.35 mm, k_c is increased a little on the contrary. The reason is that an increasing rate of J_g is greater than the one of d_b in this range. J_g is determined by the degree of containing the amount of air within the column. That is, increasing J_g increases air holdup within column. At the end of this aspect, air holdup within column becomes maximum in the range of bubble size of 0.3-0.35 mm, finally to induce the increase of flotation rate.

Fig. 10 is the collection rate constant as a function of superficial gas velocity, and this relationship is given by Eq. (18). For a given flotation system operating at a specific gas velocity and bubble size, an increase in gas velocity would be expected from Eq. (18) to yield an increase in collection rate. However, an increase in superficial gas velocity increases bubble size which reduces flotation rate constant as described in Fig. 10. Thus, flotation rate constant had a maximum in the superficial gas velocity of 1.5-2.0 cm/s. Optimum condition from this study is similar with Lee's experimental optimum condition (bubble size of 0.43 mm and superficial gas velocity of 1.99 cm/s) [Lee, 1999].

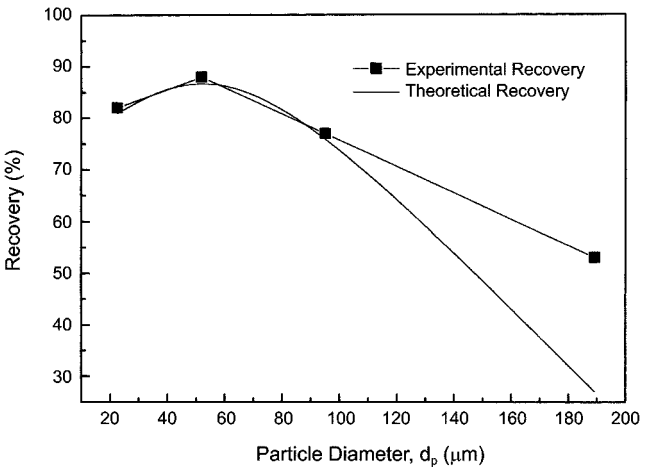

Fig. 11. Comparison of experimental and theoretical particle recovery.

3. Particle Recovery (Experimental vs. Theoretical)

Fly ash particles in the size range of below 38, 38-75, 75-125, and above 125 μm were used as separation test particles. Particles in the mass median diameter were 22.5, 52.0, 95.1 and 189.2 μm, respectively. Separation tests were performed at an optimum condition (d_b=0.34 mm, J_g=1.99 cm/s). Experimental particle recoveries were 82, 88, 77 and 53% in the particle size of 22.5, 52.0, 95.1 and 189.2 μm, respectively (as shown in equation 23). Fig. 11 is the comparison between experimental and theoretical particle recovery. Theoretical recovery obtained from Eq. (19) had a similar value as experimental recovery, but had a large difference in the particle size up to 100 μm. Thus, further study on the column flotation systems using microbubbles is needed to estimate the particle recovery with the particle size up to 100 μm.

CONCLUSIONS

A fundamental model of flotation was considered to estimate the particle recovery. Collection efficiency, flotation rate constant and particle recovery were calculated by experimental data on the bubble behavior such as bubble size, gas holdup and bubble swarm velocity. Experimental particle recovery was compared to the theoretical particle recovery.

1. Collection efficiency increased with decreasing bubble size and increasing particle size but decreased in the particle size up to 52 μm.
2. Flotation rate constant increased with decreasing bubble size but was larger in the bubble size of 0.3-0.4 mm than in that of 0.26 mm.
3. A decrease in bubble size increased collection efficiency but did not improve particle recovery.
4. Separation tests were performed at an optimum condition (d_b= 0.34 mm, J_g=1.99 cm/s). Theoretical recovery had a similar value as experimental recovery but had a large difference in the particle size up to 100 μm. Thus, further study on the column flotation systems using microbubbles is needed to estimate the particle recovery with the particle size up to 100 μm.

ACKNOWLEDGEMENTS

The authors wish to thank the Institute for Environmental Technology and Industry (IETI) and Korea Science and Engineering Foundation (KOSEF) for the financial support [R12-1996-009401-0].

NOMENCLATURE

A_c : cross section of the column [cm^2]
A_e : area of the electrode [cm^2]
C_F : concentration of the surfactant [mg/L]
D_c : diameter of the column [cm]
d_b : bubble diameter [mm]
d_p : particle diameter [μm]
E_A : attachment efficiency
E_C : collision efficiency
E_{Cg} : collision efficiency by gravitation
E_{Ci} : collision efficiency by interception
E_K : collection efficiency
F_b : buoyant force [N]

F_d : drag force [N]
F_g : gravitational force [N]
F_i : inertial force [N]
g : gravitational acceleration [m/s^2]
H_C : collection zone height [cm]
J_g : superficial gas velocity [cm/s]
K : electrical conductivity [μm]
k_C : flotation rate constant
L_e : length of the electrode [cm]
Q_a : air rate [lpm]
Re_b : Reynolds number of bubbles
R : recovery of particle
Sk : Stokes number
t_i : induction time [ms]
t_p : residence time of particle [s]
t_s : sliding time [ms]
U_s : bubble swarm velocity [cm/s]
Δh : water level difference of the manometer [cm]
ΔL : difference between manometers [cm]
ΔL_e : difference between electrodes [cm]

Greek Letters

ε_g : gas holdup
θ_c : angle of closest approach for fluid streamlines, degree
θ_m : maximum angle of contact, degree
θ' : θ that yields $t_s=t_i$
μ : liquid viscosity [dyne·s/cm]
ξ_s : surface vorticity
$\xi_{s\varepsilon}$: surface vorticity at gas holdup ε_g
ρ_l : density of liquid [g/cm^3]
ρ_p : density of particle [g/cm^3]

Subscripts

a : air
b : bubble
c : column
e : electrode
F : frother
g : gas
l : liquid
p : particle
s : swarm

REFERENCES

Bando, Y., Kuze, T., Sugimoto, T., Yasuda, K. and Nakamura, M., "Development of Bubble Column for Foam Separation," *Korean J. Chem. Eng.*, **17**, 5 (2000).

Bergh, L. G. and Yianatos, J. B., "Control Alternatives for Flotation Columns," *Minerals Engineering*, **6**, 631 (1993).

Clift, R., Grace, J. R. and Weber, M. E., "Bubbles, Drops and Particles," Academic Press, N.Y. (1978).

Dobby, G. S. and Finch, J. A., "A Model of Particle Sliding Time for Flotation Size Bubbles," *Journal of Colloid and Interface Science*, **109**, 493 (1986).

Dobby, G. S. and Finch, J. A., "Particle Collection in Columns-Gas Rate and Bubble Size Effects," *Canadian Metallurgical Quarterly*, **25**, 9 (1986).

Finch, J. A. and Dobby, G. S., "Column Flotation," Pergamon Press, Oxford, England (1990).

Hur, J. M., Chang, D. and Chung, T. H., "Characteristics of Critical Solid-Liquid Separation and Its Effect on the Performance of an Anaerobic Sequencing Batch Reactor Treating Municipal Sludge," *Korean J. Chem. Eng.*, **15**, 596 (1998)

Jiang, Z. W. and Holtham, P. N., "Theoretical Model of Collision between Particles and Bubbles in Flotation," *Trans. Instn. Min. Metall.*, **95**, C187 (1986).

Kil, J. H., Choi, J. W., Noh, K. S. and Ha, B. H., "Study on Removal of Unburned Carbon From Fly Ash by Column Flotation," *HWAHAK KONGHAK*, **37**, 719 (1999).

LeClair, B. P., Ph.D. Thesis, McMaster University, Hamilton, Ontario (1970).

Lee, D. H., Epstein, N. and Grace, J. R., "Hydrodynamic Transition from Fixed to Fully Fluidized Beds for Three-Phase Inverse Fluidization," *Korean J. Chem. Eng.*, **17**, 684 (2000).

Lee, J. E., "Separation Characteristics from Fly Ash through the Analysis of Bubble Behavior in the Liquid/Gas Flow Field," Ph.D. Thesis, Pusan National University, Pusan, Korea (1999).

Nam, S. H., Cho, Y. J., Kang, Y. and Kim, S. D., "Bubble Characteristics in Three-Phase Circulating Fluidized Beds," *HWAHAK KONGHAK*, **38**, 859 (2000).

Patel, S. A., Daly, J. G. and Bukur, D. B., "Bubble Size Distribution in Fischer-Tropsch-Derived Waxes in a Bubble Column," *AIChE Journal*, **36**, 93 (1990).

Reay, D. and Ratcliff, G. A., "Removal of Fine Particles from Water by Dispersed Air Flotation: Effects of Bubble Size and Particle Size on Collection Efficiency," *Canadian Journal of Chemical Engineering*, **51**, 178 (1973).

Sutherland, K. L., "Kinetics of the Flotation Process," *Journal of Physics and Colloid Science*, **52**, 394 (1948).

Tuteja, R. K., Spottiswood, D. J. and Misra, V. N., "Column Parameters: Their Effect on Entrainment in Froth," *Minerals Engineering*, **3**, 1359 (1995).

Uribe-Salas, A., Gomez, C. O. and Finch, J. A., "A Conductivity Technique for Gas and Solids Holdup Determination in Three-Phase Reactors," *Chemical Engineering Science*, **49**, 1 (1994).

Weber, M. E. and Paddock, D., "Interceptional and Gravitational Collision Efficiencies for Single Collectors at Intermediate Reynolds Numbers," *Journal of Colloid and Interface Science*, **94**, 328 (1983).

Woo, S. W., Ph.D. Thesis, McMaster University, Hamilton, Ontario (1971).

Yamashita, F., "Effect of Geometrical Parameters of Draft Tubes and Clear Liquid Height on Gas Holdup in a Bubble Column for Gas Dispersion into Tubes," *Korean J.Chem. Eng.*, **16**, 6 (1999).

Yianatos, J. B., Finch, J. A., Dobby, G. S. and Xu, M., "Bubble Size Estimation," *Journal of Colloid and Interface Science*, **126**, 37 (1988).

Yoon, R. H., "Microbubble Flotation," *Minerals Engineering*, **6**, 619 (1993).

Youn, J. M., Cho, Y. J., Kang, Y. and Kim, S. D., "Gas Holdup and Bubble Characteristics in Tapered Bubble Columns," *HWAHAK KONGHAK*, **38**, 864 (2000).

Zhou, Z. A., Egiebor, N. O. and Plitt, L. R., "Frother Effects on Bubble Motion in a Swarm," *Canadian Metallurgical Quarterly*, **32**, 89 (1993).